EUROPEAN ORGANIZATION FOR NUCLEAR RESEARCH

L3 Note 2592
July 1, 2000

Search for a Fermiophobic Higgs in HZ$\rightarrow$WW*$\rightarrow$($\nu\nu$)qqqq

The L3 Collaboration

Abstract

A search is performed for a Higgs boson, decaying into W bosons, using the data collected by the L3 detector at center-of-mass energies up to 209 GeV at LEP. The process $e^+e^- \rightarrow HZ \rightarrow \nu\nu WW^*$ is considered where both W bosons decay hadronically. Limits on the rate of the Higgs boson decay into W bosons as a function of the Higgs mass are presented.

Submitted to the *XXXth International Conference on High Energy Physics*
July 27 - August 2, 2000, Osaka, Japan

1 Introduction

The Standard Model has proven itself over the last 20 years to be extraordinarily effective at describing all experimental results. The Higgs boson is the most crucial unobserved part of the Standard Model(SM). In the SM, the Higgs's role is to provide masses to the W and Z bosons. Through Yukawa terms, the Higgs scalar also provides masses for the fermions as well. This model of the Higgs field is not unique. Other Higgs field constructions explain mass generation as well, but produce very different observable signatures. For example, in the general-two-doublet model one expects two scalar Higgs bosons. For certain choices of the model parameters, one of these scalars provides mass only to the fermions and the other couples exclusively to the bosons, a "fermiophobic" Higgs [1]. The masses of these two Higgs scalars might be vastly different.

To date, the search for a fermiophobic Higgs has been carried out primarily in the H$\rightarrow \gamma\gamma$ channel, where the Higgs couples to the photons through a W loop. For Higgs scalars heavier than 90 GeV, however, the branching fraction of $\gamma\gamma$ predicted relative to WW* becomes very small(See Figure 1). This motivates a search for H$\rightarrow$WW*. In most fermiophobic models, the coupling of the Z boson to the fermiophobic Higgs is not changed, so the same production process ("Higgsstrahlung") can be used for the search.

A full search of all the channels of HZ$\rightarrow$WW*(f$\bar{\text{f}}$) is at least as complicated as the regular multichannel Standard Model search. There are six different major channels (each with at least 6% of the branching ratio): qqqqqq (30%), qqqqlν (30%), $\nu\nu$qqlν (10%), llqqqq (6%), llqqlν (6%) and $\nu\nu$qqqq (10%). The last listed channel ($\nu\nu$qqqq) is the focus of the current note. The signature of this channel is particularly clean, since the invisible mass should be m_Z and there are few four-jets-plus-missing-energy processes at the LEP2 energies. The $\nu\nu$qqqq channel additionally offers direct reconstruction of the Higgs mass.

2 Data and Monte Carlo Samples

The data were collected by the L3 detector [2] in 1999 and 2000 at center-of-mass energies between 192 and 208.9 GeV. The 1999 data used (200 GeV and above) totals to 119.8 pb^{-1}. The 2000 data used for this note total 73.9 pb^{-1}, with a luminosity-averaged center-of-mass energy of 205.8 GeV.

The Higgs signal cross section and fermiophobic branching ratios are calculated using the HZHA generator. [3] For efficiency studies, Higgs events were generated using PYTHIA [4] for Higgs masses between 100 GeVand 120 GeV, with a mass step of 1 GeV. For the background studies, the following Monte Carlo programs were used: PYTHIA ($e^+e^- \rightarrow q\bar{q}(\gamma)$, $e^+e^- \rightarrow ZZ$, $e^+e^- \rightarrow Z + e^+e^-$), KORALW [5] ($e^+e^- \rightarrow WW$), and EXCALIBUR [6]($e^+e^- \rightarrow e\nu + qq$).

The L3 detector response is simulated using the GEANT 3.15 program [7], which takes into account the effects of energy loss, multiple scattering and showers in the detector. GHEISHA [8] is used to simulate hadronic interactions in the detector.

3 Selection Process

The selection process for the $\nu\nu$qqqq analysis is carried out in two stages. In a preselection stage, basic kinematic cuts are applied. These cuts require missing energy, high multiplicity both in clusters and tracks and require a missing energy vector away from the beam pipe. These cuts eliminate backgrounds from two photon processes from the data, as well an significantly reducing the other major backgrounds.

The major remaining backgrounds are from W pair production, Z pair production, and hadronic Z/γ^* processes. The WW background is particularly from the semileptonic channel, where the lepton is a tau which decays hadronically. The ZZ background is primarily $\mathrm{qq}\nu\nu$ events, which have the same recoil mass as that expected for the signal. These backgrounds are reduced by a neural network technique with separate networks trained for each background. The networks use the same eight variables, plus one additional in the case of the QQ background.

The signal is "four jets plus missing energy", and the missing or recoil mass should be $\mathrm{m_Z}$. The boosted four jet system can be reduced to a system at rest in the laboratory frame by simply deboosting the system by the visible boost. The maximum and minimum jet energies of these deboosted jets, as well as the minimum jet-jet angle in the deboosted system are powerful quantities used by the network. Additionally, the network uses the recoil mass, $\log(\mathrm{Y_{23D}})$, $\log(\mathrm{Y_{34D}})$, and the minimum and average charge track multiplicities for the four jets.

The performance of the trained networks is shown in Figure 2. One additional cut is applied to events with identified tau leptons, to eliminate the WW$\rightarrow qq\tau\nu$ background. The event is fit to two jets, subtracting the identified tau. Then, the jet energies and masses are rescaled by a common factor to make $\mathrm{E_{j1}} + \mathrm{E_{j2}} = \frac{\mathrm{E_{cm}}}{2}$, keeping $\beta \left[= \sqrt{1 - \left(\frac{m}{E}\right)^2} \right]$ constant. A selection cut is then applied on the invariant mass of the two jet system, which eliminates 30% of the remaining WW background.

The final selection has an average efficiency of 54.1%. The final mass variable is constructed by adding the visible mass to the recoil mass of the system, and subtracting $\mathrm{m_Z}$. This procedure corrects for some mismeasurement of angles and improves the resolution. The reconstructed Higgs mass has an average resolution of 4 GeV. Plots of the reconstructed mass for two different Higgs mass hypotheses are shown in Figure 3. These distributions are used for calculating confidence levels.

4 Results

The numbers of selected events after both preselection and selection for the 1999 and 2000 data and their background prediction are shown in Table 1. The expected number of events from the standard fermiophobic model is also given. No excess of data is observed. Cross-section branching ratio limits for $\sigma(\mathrm{e^+e^-} \rightarrow \mathrm{HZ})\mathrm{Br}(\mathrm{H} \rightarrow \mathrm{WW^*})$ are set at a reference center-of-mass energy $\sqrt{\mathrm{s}} = 206$ GeV. These are plotted in Figure 4. The fermiophobic prediction is shown in the figure as well.

Acknowledgements

We wish to express our gratitude to the CERN accelerator division for the excellent performance of the LEP machine. We acknowledge with appreciation the effort of the engineers, technicians and support staff who have participated in the construction and maintenance of this experiment.

References

[1] H. Haber, G. Kane and T. Sterling, Nucl. Phys. **B 161** (1979) 493; Marco A. Diaz and Thomas J. Weiler, preprint hep-ph/9401259; L. Brücher and R. Santos, preprint hep-ph/9907434; L. Brücher and R. Santos, preprint hep-ph/0002027.

[2] L3 Collab., B. Adeva *et al.*, Nucl. Instr. and Meth. **A 289** (1990) 35;
M. Chemarin *et al.*, Nucl. Instr. and Meth. **A 349** (1994) 345;
M. Acciarri *et al.*, Nucl. Instr. and Meth. **A 351** (1994) 300;
G. Basti *et al.*, Nucl. Instr. and Meth. **A 374** (1996) 293;
I.C. Brock *et al.*, Nucl. Instr. and Meth. **A 381** (1996) 236;
A. Adam *et al.*, Nucl. Instr. and Meth. **A 383** (1996) 342.

[3] P.Janot, "The HZHA generator", in "Physics at LEP2", Eds. G.Altarelli, T.Sjöstrand and F.Zwirner, CERN 96-01 (1996) Vol.2, 309.

[4] T.Sjöstrand, CERN-TH/7112/93 (1993), revised August 1995; T.Sjöstrand, Comp. Phys. Comm. 82 (1994) 74.

[5] M.Skrzypek *et al.*, Comp. Phys. Comm. **94** (1996) 216; M.Skrzypek *et al.*, Phys. Lett. **B372** (1996) 289.

[6] F. A. Berends, R. Kleiss and R. Pittau,Nucl. Phys. **B 424** (1994) 308; Nucl. Phys. **B 426** (1994) 344; Nucl. Phys. (Proc. Suppl.) **B 37** (1994) 163; Phys. Lett. **B 335** (1994) 490; R. Kleiss and R. Pittau, Comp. Phys. Comm. **83** (1994) 14.

[7] R.Brun *et al.*, preprint CERN DD/EE/84-1 (Revised 1987).

[8] H.Fesefeldt, RWTH Aachen Report PITHA 85/02 (1985).

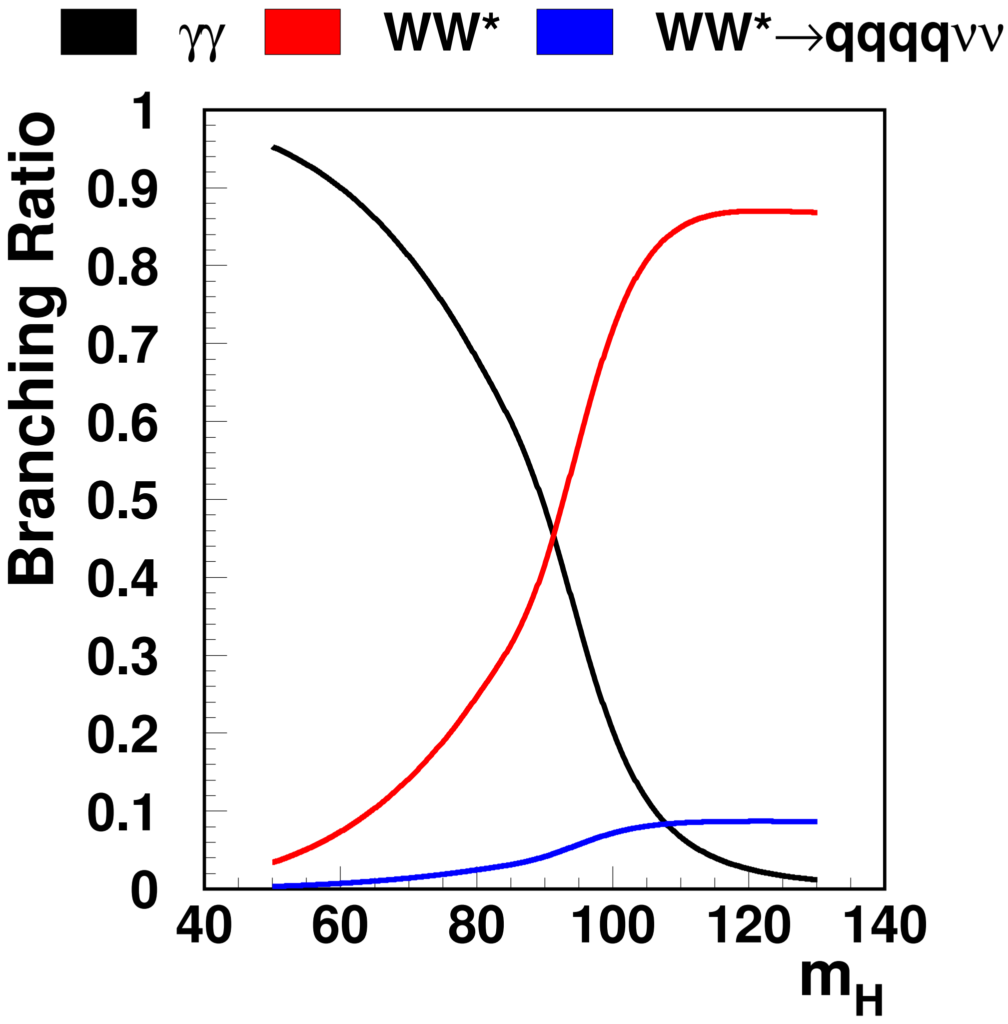

Figure 1: Branching ratio of a fermiophobic Higgs.

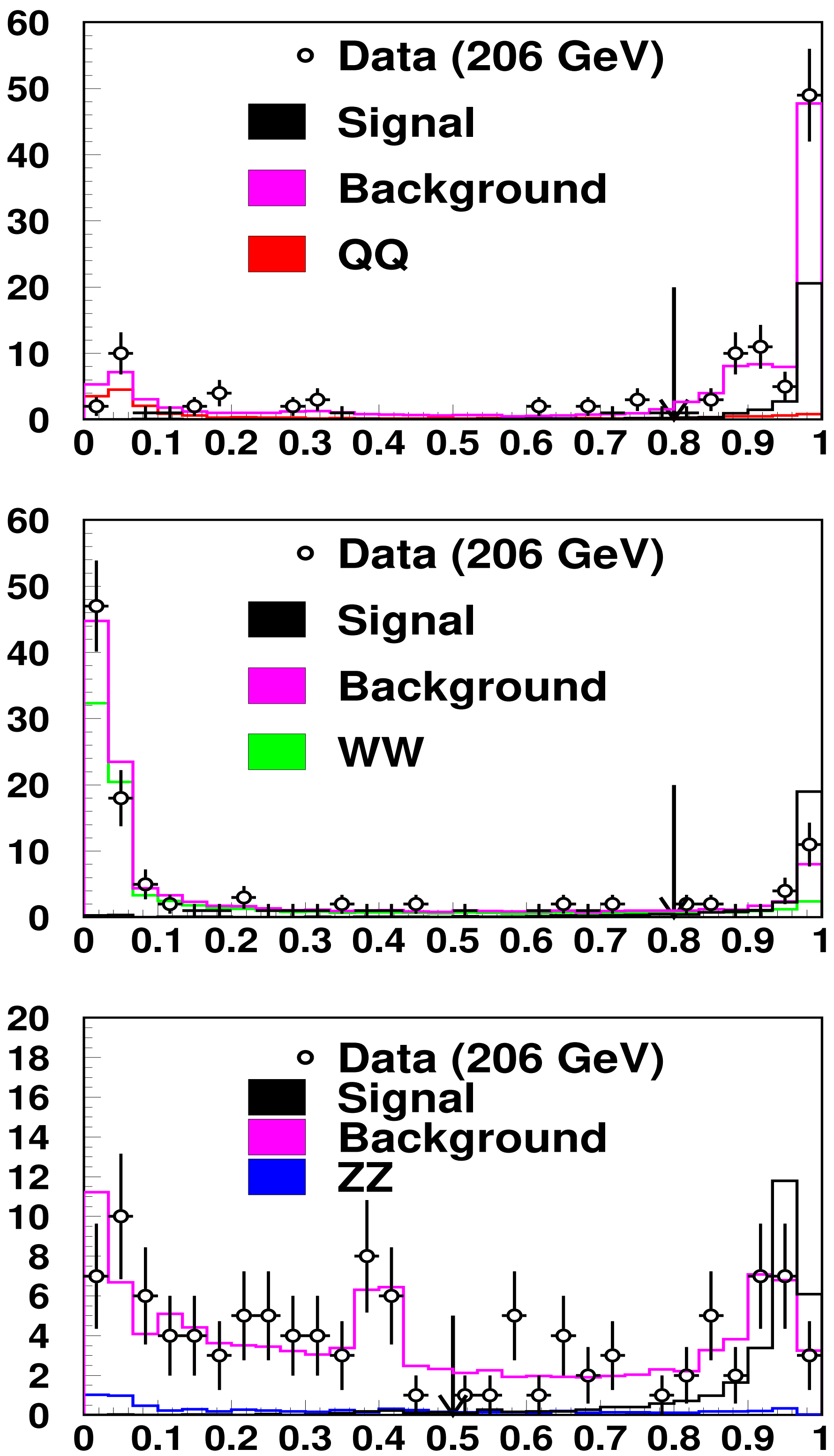

Figure 2: Performance the three neural networks used to separate signal and background. (signal in arbirary units)

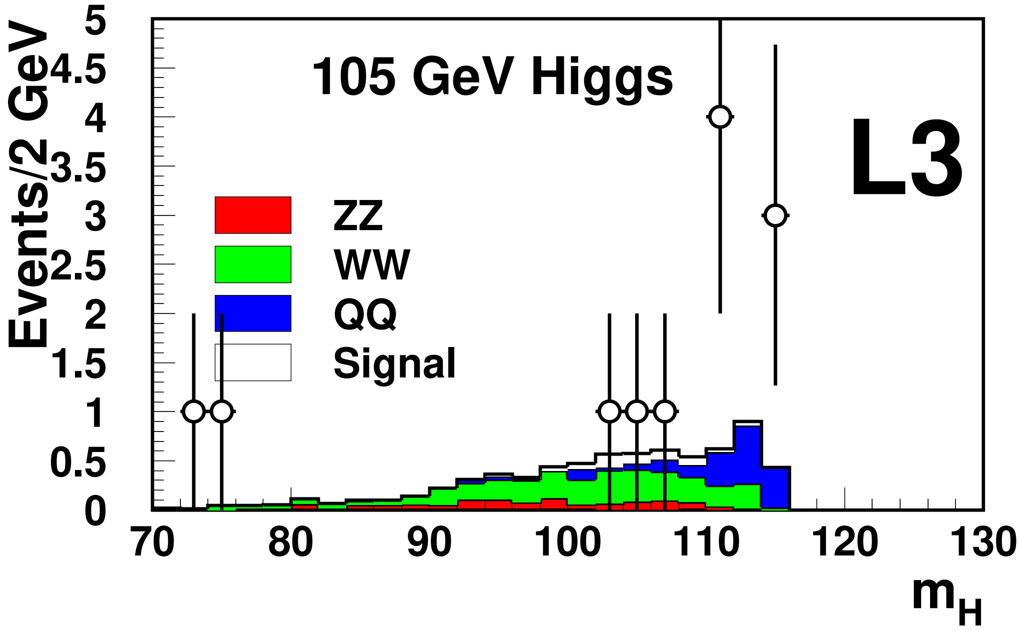

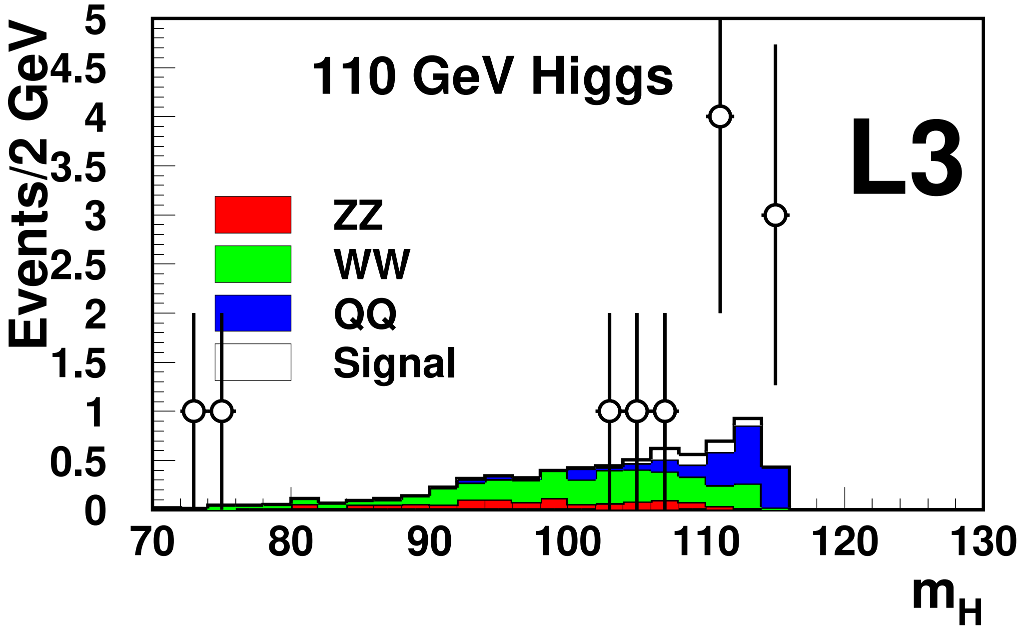

Figure 3: Final mass variable for two Higgs mass hypotheses.

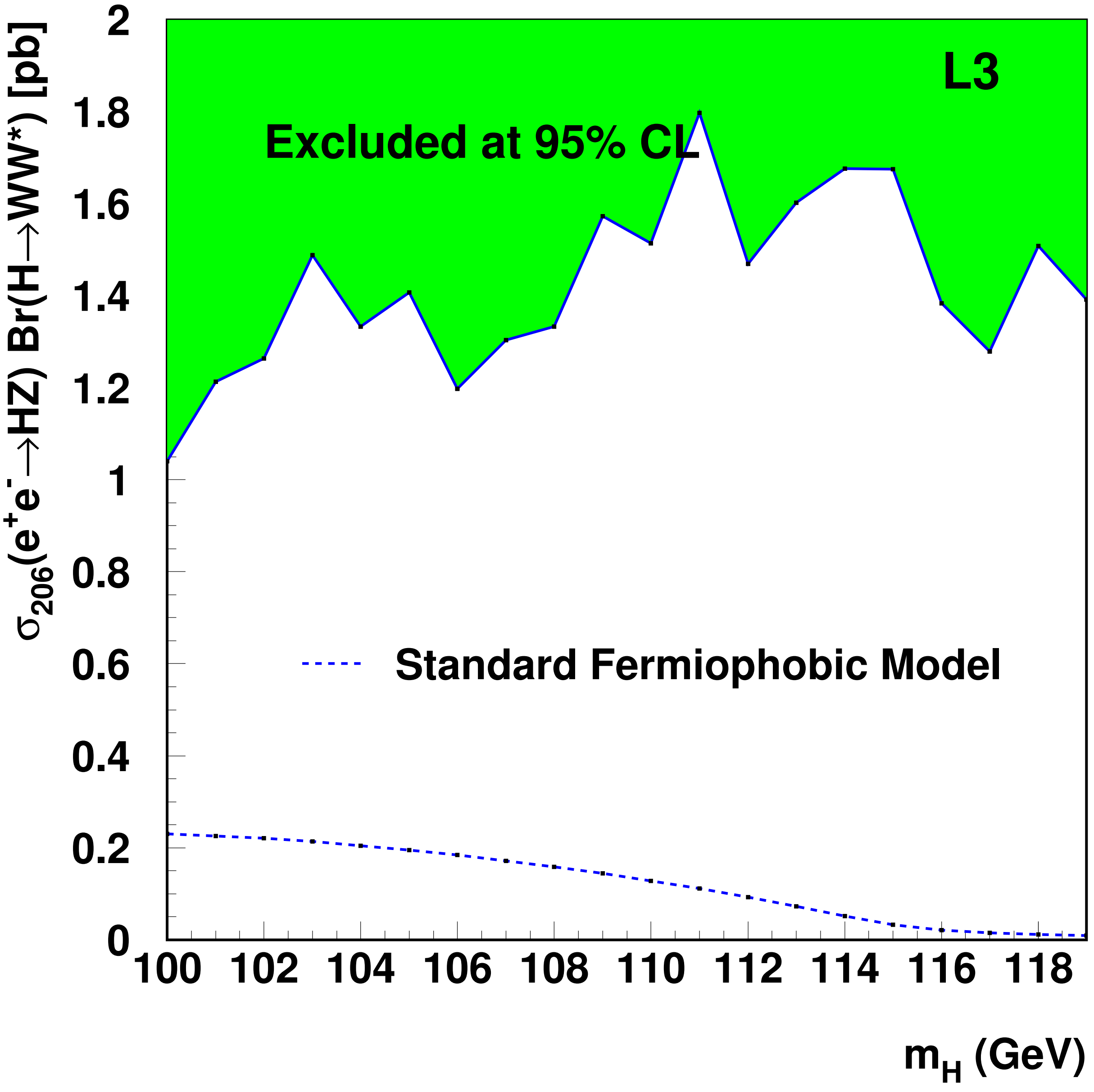

Figure 4: Cross-section branching ratio limits as a function of Higgs mass.

	2000		1999	
	Preselection	Selection	Preselection	Selection
WW Background	92.9	3.47	163.0	5.1
QQ Background	22.1	1.86	43.1	3.7
ZZ Background	8.6	1.16	12.2	2.1
W Background	6.1	0.07	10.7	0.3
Zee Background	0.6	0.28	0.9	0.0
Total Expected	130.2	6.84	229.9	11.2
Data	137	12	241	13
Signal(m_H=100)	1.48	1.06	2.18	1.53
Signal(m_H=105)	0.94	0.54	1.08	0.66
Signal(m_H=110)	0.54	0.41	0.22	0.17
Signal(m_H=115)	0.18	0.12	0.07	0.05

Table 1: Preselection and Selection for 1999 and 2000